Theor Chem Acc (2011) 130:555–561
DOI 10.1007/s00214-011-1056-z

REGULAR ARTICLE

Understanding properties of copoly(arylene ether nitrile)s high-performance polymer electrolyte membranes for fuel cells from molecular dynamics simulations

Takahiro Ohkubo · Yasuhiko Iwadate · Yu Seung Kim · Neil Henson · Yoong-Kee Choe

Received: 27 August 2011 / Accepted: 22 September 2011 / Published online: 4 October 2011

Abstract Sulfonated poly(arylene ether ether nitrile) (m-SPAEEN) copolymers are reported to have the property of reduced water uptake compared with other hydrocarbon membranes, such as sulfonated polysulfones or polyketones, with similar ion exchange capacity. It is believed that this difference is largely due to the nitrile group. In this study, to investigate the effect of the nitrile group on properties of polymer electrolyte membranes for fuel cell applications, we carried out a series of molecular dynamics (MD) simulations. We compared the results of MD simulations for m-SPAEEN and sulfonated poly(arylene ether sulfone)s (BPSH). We found that water molecules hydrate not only the sulfonate (SO_3^-) groups of m-SPAEEN but also other hydrophilic functional groups in the copolymers. Results showed that hydration around the nitrile group in m-SPAEEN and around the sulfone (SO_2) group in BPSH differs in features related to water uptake: The former exhibits uptake of fewer water molecules than does the latter. This difference in hydration features causes m-SPAEEN to have a relatively low water-uptake level compared with BPSH.

Keywords Polymer electrolyte membrane · Fuel cell · Molecular dynamics simulation

Dedicated to Professor Shigeru Nagase on the occasion of his 65th birthday and published as part of the Nagase Festschrift Issue.

T. Ohkubo · Y. Iwadate
Department of Applied Chemistry and Biotechnology, Chiba University, Chiba-shi, Chiba 263-8522, Japan

Y. S. Kim
Material Physics and Applications, Sensors and Electrochemical Devices Groups, Los Alamos National Laboratory, Los Alamos, NM 87544, USA

N. Henson
Physics and Chemistry of Materials, Los Alamos National Laboratory, Los Alamos, NM 87544, USA

Y.-K. Choe (✉)
Nanosystem Research Institute, National Institute of Advanced Industrial Science and Technology, Tsukuba 305-8564, Japan
e-mail: yoongkee-choe@aist.go.jp

1 Introduction

Polymer electrolyte fuel cells (PEFCs) are actively being developed because of their potential applications in portable and stationary systems [1]. An important component of a PEFC is the polymer electrolyte membrane (PEM), whose role is to facilitate proton conduction and to separate the anode and the cathode. It has been suggested that PEMs should have high proton conductivity, good mechanical and chemical stability under fuel cell operation conditions and low production cost [2]. Perfluorinated acid-type polymers, such as Nafion, are widely used for PEFCs because of their excellent proton conductivity and good mechanical and chemical stability [3]. Although Nafion is a good polymer for PEFC applications, it does have several shortcomings, such as high production cost, high methanol permeability and low operating temperature (<80 °C), which has prompted the development of new membranes.

Hydrocarbon-based polymers have attracted considerable attention as alternatives. The cost of hydrocarbon PEMs is generally lower than that of perfluorinated ones [4]. Typical examples of hydrocarbon-based polymers are sulfonated aromatic polymers, such as sulfonated poly (ether ether ketones) (SPEEKs) [5]. Most such aromatic polymers exhibit poor proton conductivity when the water content is low, compared with Nafion [6]. This property

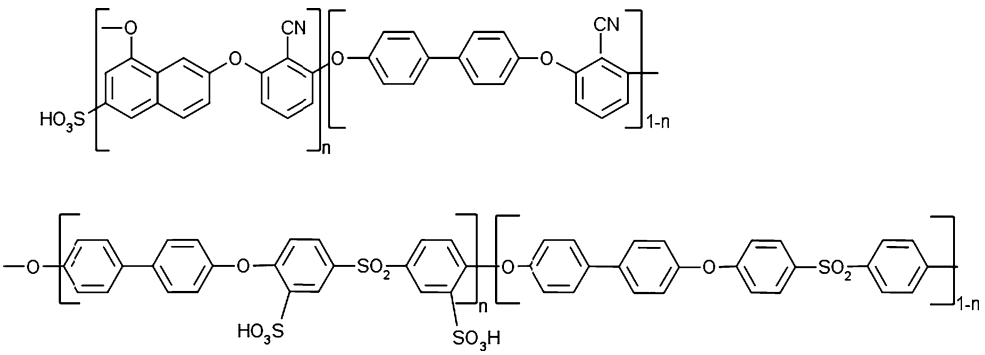

Fig. 1 Molecular structure of m-SPAEEN and BPSH (*n* refers to the mole ratio of a sulfonated monomer to a nonsulfonated one)

Table 1 The numbers of H_2O and H_3O^+ and polymer chains used in the simulated systems

Monomer	Polymer	H_3O^+	H_2O	λ	Box size (Å)	Wt (%)	Particle number
m-SPAEEN-50	15	150	1,050	8.0	50.02	23	14,100
m-SPAEEN-60	15	180	1,278	8.1	55.52	28	14,874
BPSH-35	15	210	2,520	12.6	61.33	35	23,130

is one of the major drawbacks of hydrocarbon-based polymers because it is desirable to operate a PEFC under conditions of low hydration or no water conditions, in order to avoid the requirement for water management. Therefore, to obtain satisfactory proton conductivity for fuel cell applications, suitable polymers require a higher degree of sulfonation [7]. However, an increase in the degree of sulfonation generally also results in excess water uptake by hydrocarbon membranes. Such excess water swelling subsequently results in deterioration of the performance of the membranes for fuel cell applications because of their mechanical fragility [8]. Thus, the question arises as to how to design a polymer that retains low water uptake at a very high degree of sulfonation.

Recently, sulfonated aromatic polymers having a nitrile moiety draw attention since these copolymers exhibited reduced water uptake compared with typical sulfonated aromatic membranes, such as sulfonated polyether sulfones or polyketones, with similar ion exchange capacity (IEC) [9]. This property of reduced water uptake is very important for fuel cell applications because it allows increased incorporation of sulfonic acid groups into polymers without an excessive increase in water uptake. Furthermore, membranes made from nitrile copolymers exhibit excellent methanol impermeability that is beneficial to direct methanol fuel cells. It has been suggested that the nitrile groups in the sulfonated polymers play an important role in the reduced water-uptake property [9, 10]. However, the origin of this on a molecular level has not yet been elucidated.

In this study, we carried out molecular dynamics (MD) simulations to investigate the structural aspects and details of the water-uptake property of the water-swollen nitrile copolymers. To date, MD simulations have been successfully applied to various PEMs, including Nafion and hydrocarbon membranes [11–28], and several review articles on this subject have been published [29–31]. These simulations provide information regarding structural features of water-swollen PEMs and various transport properties, which, by compensating experimental observations, provides deeper understanding of the physics and chemistry of PEMs. In this paper, we present the results of MD simulations carried out for sulfonated poly(arylene ether ether nitrile) (m-SPAEEN) copolymers and sulfonated poly(arylene ether sulfone)s (BPSH), the chemical structures of which are depicted in Fig. 1. The MD simulation for BPSH was conducted for comparison purposes.

2 Computational details

Table 1 gives details of the molecular models employed in the present study. MD simulations were carried out for three polymer systems: m-SPAEEN-50, m-SPAEEN-60 and BPSH-35. In m-SPAEEN-50, "50" indicates that the two repeat units in the copolymer are present in an equal ratio (n/1–n = 50:50); in m-SPAEEN-60, "60" means that the ratio is 60:40. A similar notation applies for BPSH-35. The hydration level (λ), which is defined as the number of water molecules per sulfonic group, corresponds to experimental values obtained at full equilibration in water.

To maintain the neutrality of the system, H_3O^+ was used as the counterion to SO_3^-. The force field selected for this study was a simplified consistent force field, which is a second-generation force field [32]. It has been successfully applied to various polymer systems, including PEMs for fuel cells [33–35]. Missing force field parameters were

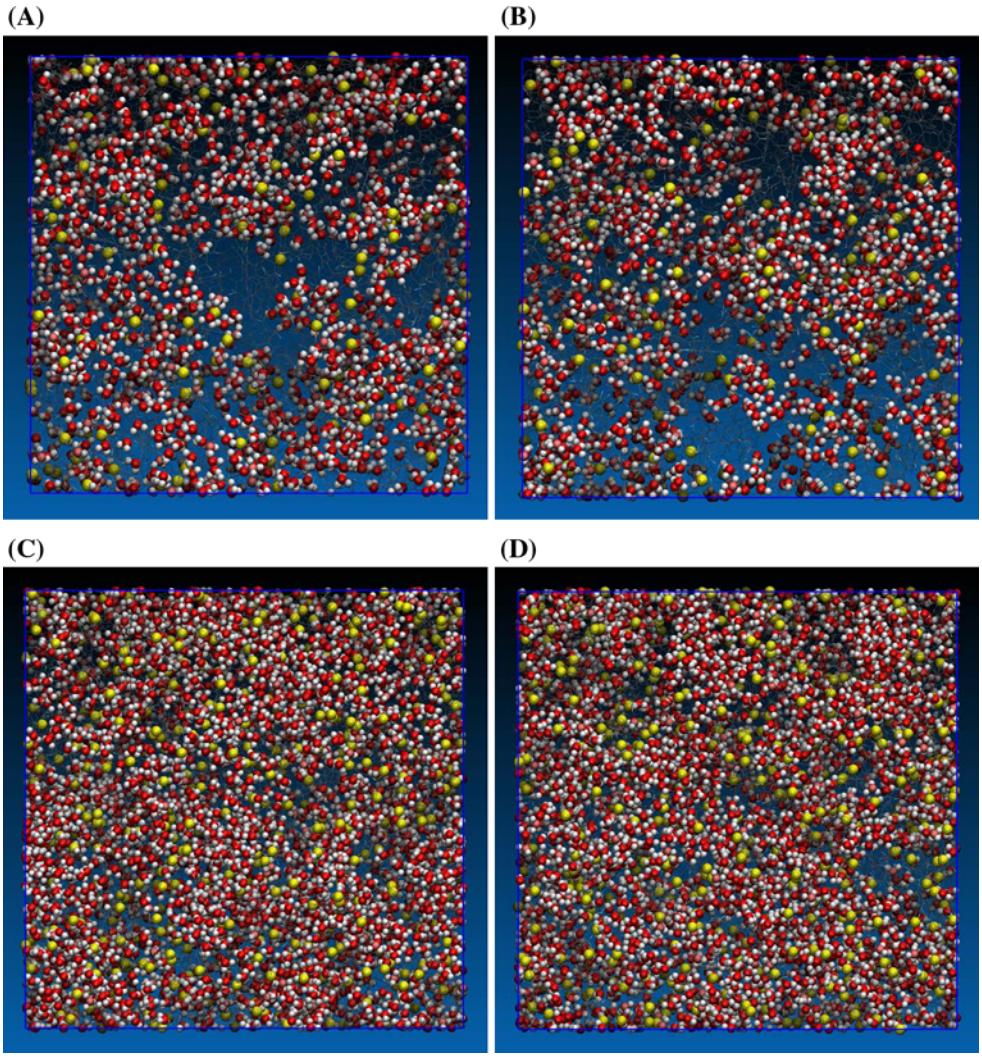

Fig. 2 Snapshots from trajectories. *Gray lines*, polymer backbone; *red balls*, oxygen atom of H_2O; *pink ball*, oxygen atom of H_3O^+; *white ball*, hydrogen atoms; *yellow ball*, sulfur atoms. *Blue lines* are periodic boundaries of the unit cell. **a** m-SPAEEN-50, *front view*; **b** m-SPAEEN-50, *side view*; **c** BPSH-35, *front view;* **d** BPSH-35, *side view*

assigned following the method developed by Sato et al. [36]. Classical MD simulations were carried out with the LAMMPS code [37]. Equations of motion were integrated using the Verlet algorithm with a time step of 1.0 fs, and the particle–particle particle–mesh method was employed to calculate electrostatic interactions. The initial configuration of each system was constructed using the *Amorphous Builder* module in the MAPS software package [38]. We then carried out a thermal annealing procedure five times between 298 and 800 K.

After the annealing procedure, MD simulations were performed in the NVT ensemble at 293 K for 10 ns. Trajectories obtained from the last 5 ns were used to compute the structural properties. Note that in our simulations, proton dissociation and hopping were disallowed; only the vehicular-type proton transport was taken into consideration. Snapshots from the trajectories can be seen in Fig. 2.

3 Results and discussion

3.1 Sulfonate group–water/hydronium ion interaction

In general, the sulfonate group plays a major role in water uptake in PEMs. Hence, we investigated the coordination of the water or hydronium ions around the sulfonate group. Figure 3 shows the coordination number of water molecules around the sulfonate group as a function of distance, which was computed by integrating the radial distribution function (RDF) for an atomic pair between the oxygen atom of water molecules and the sulfur atom of the sulfonate group. As shown in the figure, the coordination number of water molecules increases gradually with respect to the S–O distance.

The coordination numbers at 4.5 Å are 4.7, 5.1 and 6.0 for m-SPAEEN-50, m-SPAEEN-60 and BPSH-35,

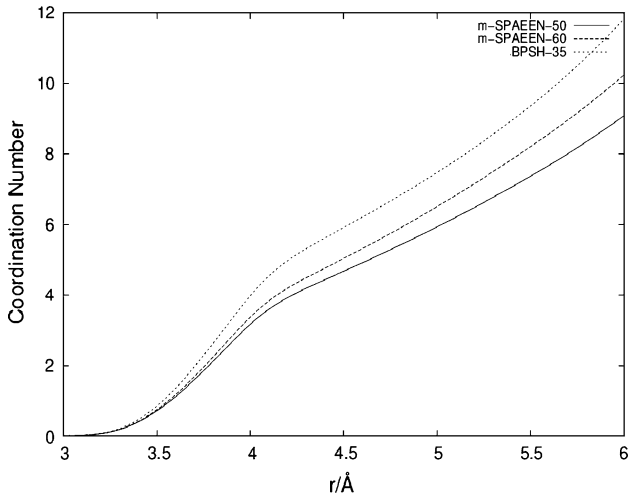

Fig. 3 Coordination number of water around SO_3^- as a function of distance

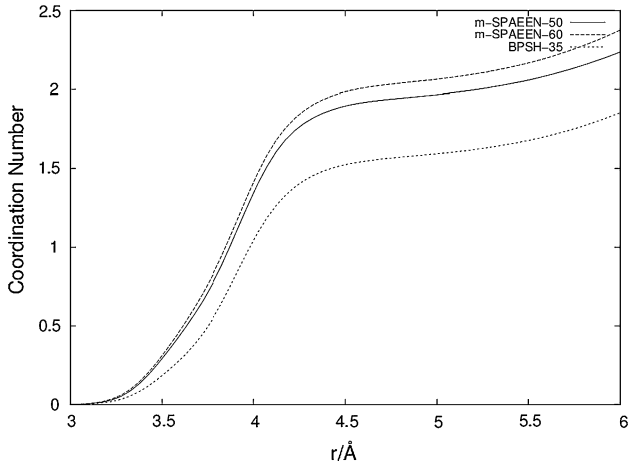

Fig. 4 Coordination number of a hydronium ion around SO_3^- as a function of distance

respectively. The value of 4.5 Å is a typical cutoff distance for counting the number of water or hydronium ions around the sulfonate group. The uptake of BPSH-35 is about one water molecule more than that of the SPAEEN copolymers. The data also show that the coordination number is proportional to the IEC value (BPSH-35 > m-SPAEEN-60 > m-SPAEEN-50).

Figure 4 shows the coordination number of hydronium ions around the sulfonate group as a function of distance. It is notable that the coordination number does not increase significantly after 4.5 Å, which is in contrast to the gradual increase in the coordination number of water molecules, as presented in Fig. 3. This result indicates that one hydronium ion is located next to the sulfonate group but the second one is located far from the sulfonate group. This is a general trend; it is found in other PEMs [28, 39]. Under higher hydration conditions, water molecules in PEMs can strongly screen the hydronium ion–sulfonate interaction, which enables hydronium ions to diffuse away from the sulfonate group. The coordination numbers of hydronium ions are 1.9, 2.0 and 1.5 for m-SPAEEN-50, m-SPAEEN-60 and BPSH-35, respectively. These values are larger than 1.0, which indicates that one hydronium ion is shared by two neighboring sulfonate groups. The result is interesting because this configuration, which is sometimes referred to as a *bridged configuration*, typically occurs under low hydration conditions [28, 39], and it is indicative of the PEM being folded to a large extent. For example, the coordination numbers of hydronium ions around the sulfonate group in SPEEK are reported to be 1.4 ($\lambda = 4.9$) and 1.2 ($\lambda = 1.2$) [28]. This comparison with SPEEK may suggest that m-SPAEEN tends to favor folded configurations, even in the case of a relatively higher water content, such as $\lambda = 8.0$.

Taking the above results into consideration, the coordination numbers of water molecules plus hydronium ions were calculated to be 6.6, 7.0 and 7.5 for m-SPAEEN-50, m-SPAEEN-60 and BPSH-35, respectively. The sulfonate group in BPSH-35 absorbs about one more water molecule or hydronium ion than that in m-SPAEEN-50 and m-SPAEEN-60.

A sulfonate group's ability to absorb water molecules (including hydronium ions) is rather independent of the membranes described here, considering the difference of λ values. It is therefore logical to consider other effects that contribute to the water-uptake property. Those membranes have hydrophilic functional groups other than the sulfonate group, and because these functional groups are able to form hydrogen bonds with water molecules, the water-uptake ability of such functional groups also should be taken into account.

3.2 Nitrile/sulfone group–water interaction

Figure 5 shows the RDF for an atomic pair between the nitrogen atom of the nitrile group in m-SPAEEN-50 and m-SPAEEN-60 and the oxygen atom of H_2O. The first peak shown in the RDF arises mainly from hydrogen bonds between the nitrile group and water molecules. Also, as a previous study on acetonitrile–water mixtures indicates [40], water molecule can interact with the nitrile group through dipole–dipole interaction. The coordination number of water molecules around the nitrile group was calculated to be 2.0, with a 4.5 Å cutoff for integration. This result suggests that, in addition to the water-uptake contribution of the sulfonate group, in m-SPAEEN membranes, the nitrile group also exhibits some water uptake. Furthermore, Fig. 6, which depicts the RDF for an atomic pair between the nitrogen atom of the nitrile group and the oxygen atom of hydronium ions, shows that the nitrile

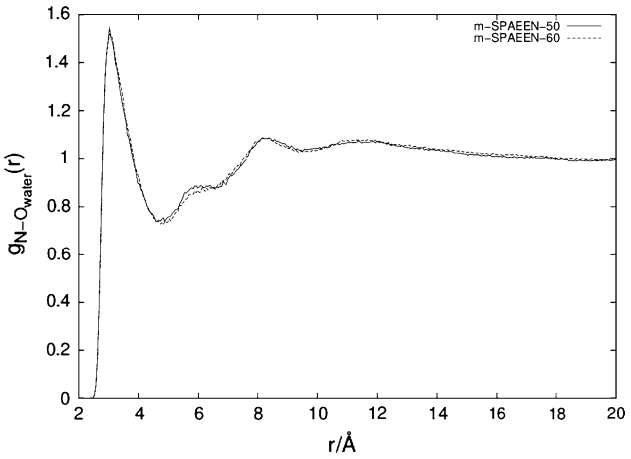

Fig. 5 RDF for an atomic pair between the nitrogen atom of the nitrile group of m-SPAEEN polymers and the oxygen atom of water molecules

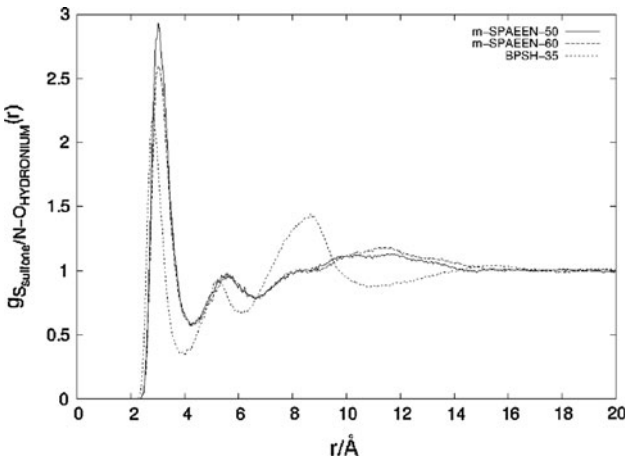

Fig. 6 RDF for an atomic pair between the nitrogen atom of the nitrile group of m-SPAEEN polymers and the oxygen atom of hydronium ions and for an atomic pair between the sulfur atom of the sulfone group of BPSH-35 and the oxygen atom of hydronium ions

group is able to form hydrogen bonds with hydronium ions. This result implies that the nitrile group can act as a proton-trapping site, which may hinder efficient proton transport in the membranes. The above implication is also true for BPSH-35, because the sulfone group of BPSH-35 forms hydrogen bonds with hydronium ions (as seen in Fig. 6).

Figure 7 shows the RDF for an atomic pair between the oxygen atom in the sulfone group and the oxygen atom of water molecules for BPSH-35. The first peak arises from the water–sulfone hydrogen bond in the water-swollen BPSH-35. The coordination number of water molecules around the oxygen atom of the sulfone group was calculated to be 2.7, with a 4.5 Å cutoff. Thus, one sulfone group is able to hold up to about five water molecules. The sulfone group of BPSH-35 is able to absorb twice as many water molecules as the nitrile group of m-SPAEEN membranes. The above results suggest that the difference in the water-uptake property between m-SPAEEN and BPSH-35 arises, in part, from the difference between water-uptake ability of the nitrile group and that of the sulfone group, although effects arising from differences in water morphology between the two types of membrane cannot be totally neglected.

3.3 Morphological aspects

In the previous sections, we explained the difference in water-uptake ability between m-SPAEEN and BPSH in terms of the difference in water-uptake ability between the nitrile and sulfone groups. It is well known that Nafion membranes are able to absorb more water molecules than typical hydrocarbon membranes, although Nafion does not have hydrophilic functional groups such as carbonyl or sulfone groups that can interact strongly with water molecules. It is also known that hydrophilic phases and hydrophobic phases tend to be strongly separated in Nafion. The case of Nafion indicates that the hydrophilic–hydrophobic phase separation that allows water molecules to form wide water channels is a very important feature affecting the water-uptake property.

Thus, to understand this morphological aspect in the membranes under discussion, we investigated the correlation between sulfur atoms of the sulfonate groups. Figure 8 shows the RDF between the sulfur atoms of SO_3^-. The first peaks of m-SPAEEN-50 and m-SPAEEN-60 are located at virtually the same position, whereas those of BPSH-35 are located at a slightly different position. In general, the S–S distance of PEMs increases with an increase in water content [28, 39], such that the difference reflects, to some extent, the difference in the water content of the membranes ($\lambda = 12.6$ for BPSH-35, and 8.0 and 8.1 for m-SPAEEN-50 and m-SPAEEN-60, respectively). Furthermore, the S–S distance is affected by the chemical structure of the two membranes. As seen in Fig. 1, BPSH-35 has two sulfonate groups in one repeat unit, whereas m-SPAEEN has one sulfonate group in the naphthalene unit. Therefore, the S–S correlation in BPSH-35 can arise from an intra-unit S–S contribution, whereas such an intra-unit S–S correlation is missing in the case of m-SPAEEN. Since the shorter average S–S distance implies more disperse and narrower water channels inside PEMs [35], the above RDF indicates that water channels inside m-SPAEEN polymers are smaller than those inside BPSH-35.

To gain further insight into the water channels inside PEMs, we carried out a cluster analysis of water, the results of which are presented in Fig. 9. In this analysis, we identified clusters of water molecules connected by a hydrogen bond network in all snapshots. The number of water molecules in each cluster was then extracted, and the

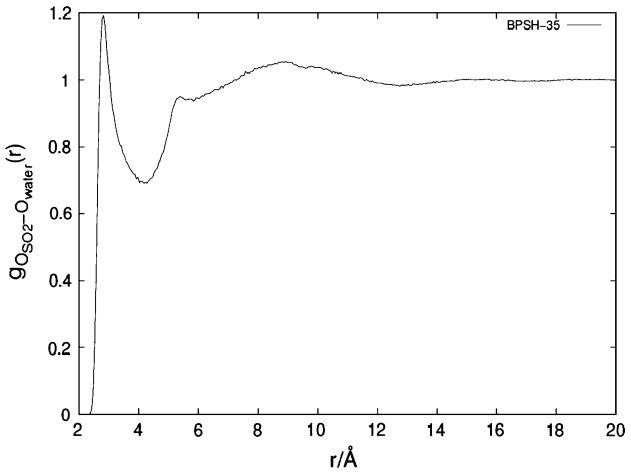

Fig. 7 RDF for an atomic pair between the oxygen atom of the sulfone (SO_2) group and the oxygen atom of water molecules

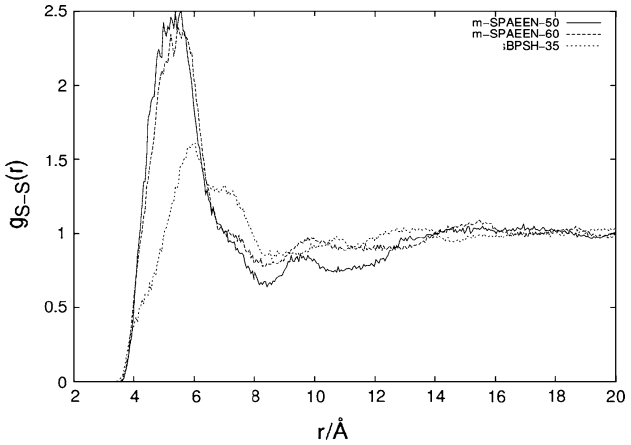

Fig. 8 RDF for an atomic pair between the sulfur atoms of the sulfonate groups

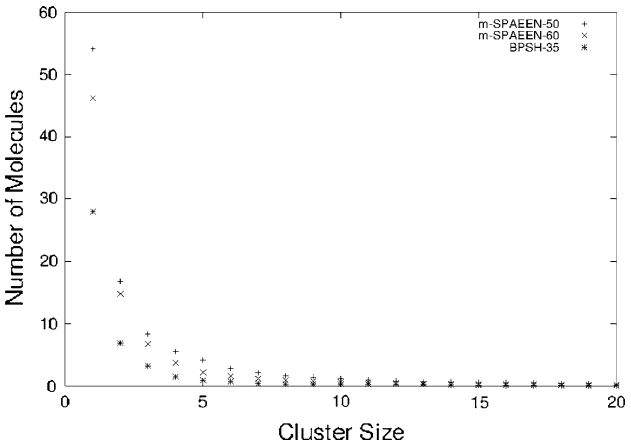

Fig. 9 Cluster distribution of water

average population of each size of cluster was calculated. Fig. 9 shows that the population of small water clusters is smaller in BPSH-35 than in m-SPAEEN-50 and m-SPAEEN-60. It is also noted that the population is inversely proportional to the IEC value. This trend is in accordance with our previous simulation results on sulfonated poly(ether sulfone) [35]. Because the population of small water clusters increases with an increase in disconnectivity of water channels inside PEMs, the above analysis indicates that the water channels inside BPSH-35 are slightly larger than those inside m-SPAEEN-50 and m-SPAEEN-60, although the difference in water cluster distribution is not great, as can be inferred from Fig. 9.

Our simulation suggests that in an environment where water cluster size distribution is not significantly different and hydrophilic–hydrophobic phase separation is not as profound as in Nafion, other effects such as the water-uptake ability of hydrophilic functional groups influence the water-uptake property of membranes.

4 Conclusions

The results of MD simulations carried out for m-SPAEEN and BPSH-35 are presented. We found that hydrophilic functional groups affect the water-uptake property of PEMs. The nitrile group in m-SPAEEN copolymers absorbs up to about two water molecules. On the other hand, the sulfone group in BPSH-35 is able to absorb more than five water molecules. Our simulations reveal that the differences in hydrophilic functional groups' ability to hold water molecules result in different PEMs having different water-uptake properties.

Acknowledgments The authors thank Professor Jim McGrath (Virginia Tech) and Dr. Michael Guiver (Canada NRC) for providing sulfonated copolymer samples. This study was supported in part by the Ministry of Industry, Economy and Trade (METI), Japan, and a grant from the New Energy and Industrial Technology Development Organization (NEDO), Japan.

References

1. Barbir F (2005) PEM fuel cells: theory and practices. Elsevier, Burlington
2. Rikukwa R, Sanui K (2000) Prog Polym Sci 25:1463
3. Mauritz KA, Moore RB (2000) Chem Rev 104:4535
4. Hickner MA, Ghassemi H, Kim YS, Einsla BR, McGrath JE (2004) Chem Rev 104:4587
5. Kreuer KD (2001) J Membr Sci 185:29
6. Hickner MA, Pivovar BS (2005) Fuel Cells 5:213
7. de Araujo CC, Kreuer KD, Schuster M, Portale G, Mendil-Jakani H, Gebel G, Maier J (2009) Phys Chem Chem Phys 11:3305
8. Norsten TB, Guiver MD, Murphy J, Astill T, Navessin T, Holdcroft S, Frankamp BL, Rotello VM, Ding J (2006) Adv Funct Mater 16:1814

9. Kim YS, Kim DS, Liu B, Guiver BD, Pivovar BS (2008) J Electrochem Soc 155:B21
10. Kim YS, Kim DS, Guiver MD, Pivovar BS (2011) J Memb Sci 374:49
11. Venkatnathan A, Devanathan R, Dupuis M (2007) J Phys Chem B 111:7234
12. Devanathan R, Venkatnathan A, Dupuis M (2007) J Phys Chem B 111:13006
13. Devanathan R, Venkatnathan A, Dupuis M (2007) J Phys Chem B 111:8069
14. Cui ST, Liu JW, Selvan ME, Paddison SJ, Keffer DJ, Edwards BJ (2008) J Phys Chem B 112:13273
15. Cui ST, Liu JW, Selvan ME, Keffer DJ, Edwards BJ, Steele WV (2007) J Phys Chem B 111:2208
16. Dokmaisrijan S, Spohr E (2006) J Mol Liq 129:92
17. Blake NP, Mills G, Metiu H (2007) J Phys Chem B 111:2490
18. Blake NP, Petersen MK, Voth GA, Metiu H (2005) J Phys Chem B 109:24244
19. Brandell D, Karo J, Liivat A, Thomas JO (2007) J Mol Model 13:1039
20. Vishnyakov A, Neimark AV (2000) J Phys Chem B 104:4471
21. Vishnyakov A, Neimark AV (2001) J Phys Chem B 105:7830
22. Jang SS, Goddard WA III, Kalani MYS, Myung D, Frank CW (2007) J Phys Chem B 111:14440
23. Jang SS, Goddard WA III, Kalani Y (2007) J Phys Chem B 111:1729
24. Jang SS, Goddard WA III (2006) J Phys Chem B 110:7992
25. Jang SS, Lin S-T, Maiti PK, Blanco M, Goddard WA III, Shuler P, Tang Y (2004) J Phys Chem B 108:12130
26. Petersen MK, Voth GA (2006) J Phys Chem B 110:18594
27. Petersen MK, Hatt AJ, Voth GA (2008) J Phys Chem B 112:7754
28. Brunello G, Lee SG, Jang SS, Qi Y (2009) J Renew Sustain Energy 1:033101
29. Paddison SJ (2003) Annu Rev Mater Res 33:289
30. Kreuer KD, Paddison SJ, Spohr E, Schuter M (2004) Chem Rev 104:4637
31. Elliott JA, Paddison SJ (2007) Phys Chem Chem Phys 9:2602
32. Maple JR, Hwang MJ, Stockfisch TP, Dinur U, Waldman M, Ewig CS, Hagler AT (1994) J Comput Chem 15P:162
33. Pozuelo J, Riande E, Saiz E, Compan V (2006) Macromolecules 25:8862
34. Hu N, Chen R, Hsu A (2006) Polym Int 55:872
35. Ohkubo T, Kidena K, Takimoto N, Ohira A (2011) J Mol Model 17:739
36. Sato F, Hojo S, Sun H (2003) J Phys Chem A 107:248
37. Plimpton S (1995) J Comput Phys 117:1
38. SARL Scienomics (2002) MAPS, version 3.1. Scienomics SARL, Paris
39. Roberto DL, Devanathan R, Dupuis M (2011) J Phys Chem B 115:1817
40. Bakó I, Megyes T, Pálinkas G (2005) Chem Phys 316:235